

Characterization of TiO₂-Doped Yttria-Stabilized Zirconia (YSZ) for Supercritical Water-Cooled Reactor Insulator Application

F. Barrett, X. Huang, and Dave Guzonas

(Submitted May 25, 2012; in revised form January 25, 2013)

In this study, TiO₂-doped YSZ samples were tested in supercritical water (SCW) to evaluate their corrosion behavior. The doped samples were produced by mechanically alloying standard 7 wt.% Y₂O₃-ZrO₂ with 5, 10, and 15 wt.% of TiO₂ first. The bulk sample pieces were then obtained using plasma spraying of the alloyed powder materials followed by sintering. The results showed that the weight changes for 5TiYSZ and 10TiYSZ after 1000 h of exposure in SCW were negligible and the sample surfaces did not exhibit any indication of corrosion. In comparison to the reference materials (Al₂O₃ and 7YSZ) processed using the same method, the rate of weight change followed the order of Al₂O₃ > 7YSZ, 15TiYSZ > 10TiYSZ > 5TiYSZ. As several TiO₂-doped 7YSZ compositions also display increased fracture toughness and reduced thermal conductivity, they may be considered as potential candidates for thermal insulation in a SCW-cooled nuclear reactor.

Keywords ceramic materials, corrosion, material for supercritical water-cooled nuclear reactor (SCWR), plasma spraying

1. Introduction

Supercritical water ($T_c=374$ °C and $P_c=22.1$ MPa) is becoming increasingly important in recent years as a fluid for energy generation and the disposal of bio-hazardous materials. It can convert biomass into combustible gasses in a supercritical water gasification process (SCWG) (Ref 1) and is also capable of oxidizing various types of toxic bio-waste in a supercritical water oxidation process (SCWO) (Ref 2). Additionally, to increase the thermodynamic efficiency of conventional nuclear-powered steam turbines, the use of supercritical water as working fluid has been proposed in a new generation of supercritical water-cooled nuclear reactors (SCWR) (Ref 3).

Canada is a member of an international consortium in the development of next generation (Gen IV) nuclear power reactors. Among the six reactor technologies selected for research and development under the Gen IV program, Canada has chosen to focus on the SCWR design. The proposed reactor outlet temperature for the

Canadian SCWR is estimated to be at or over 625 °C (Ref 4) under an operating pressure of 25 MPa. The use of high temperature supercritical water as working fluid allows a high thermodynamic efficiency that is close to 50%, compared to about 35% for an advanced Light Water Reactor (LWR). Due to the elevated temperature of SCWR coolant in the reactor core, an insulation material must be placed between the pressure tube and liner as shown in Fig. 1 (Ref 5, 6). This layout represents the most recent Canadian SCWR core design where the insulator inside the pressure tube provides temperature reduction (from up to 650 °C of SCW coolant to below 100 °C) to the pressure tube made of Zr alloy(s). The insulator thickness and properties must be optimized to allow heat loss by conduction/convection to the heavy water moderator under normal operation and sufficient heat rejection by radiation/conduction/convection under accident conditions.

The thermal insulating materials for SCWR application must be corrosion resistant to SCW at various temperatures. They should also have low thermal conductivity in order to provide the required insulation. Resistance to thermal cycling and dimensional stability under irradiation condition are additional attributes of the insulation material chosen. Surveying the open literature, limited information was found on the performance of ceramic materials in SCW (Ref 7-13). In general, oxide-based ceramics exhibited better corrosion resistance in SCW than non-oxide-based ceramic materials. The use of yttria-stabilized zirconia (YSZ) coatings on Boiling Water Reactor (BWR) piping has been shown to minimize intergranular stress corrosion cracking of sensitized stainless steel by reducing the oxygen transport rate to the

F. Barrett and X. Huang, Department of Mechanical and Aerospace Engineering, Carleton University, Ottawa, ON Canada; and Dave Guzonas, Atomic Energy Canada Laboratory, Chalk River, ON Canada. Contact e-mail: xhuang@mae.carleton.ca.

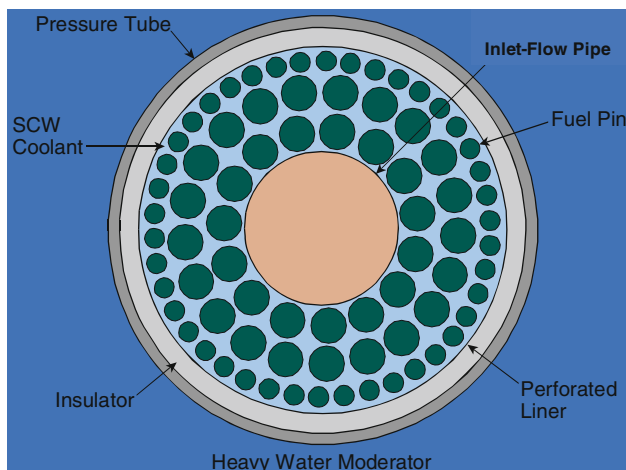


Fig. 1 Schematic diagram showing a cross section of the SCWR core design (Ref 5)

surface (Ref 7, 8). Zirconia coatings also reduced the corrosion rate of carbon and stainless steels in SCW (Ref 9, 10). In a short-term study of β -SiAlONs in SCW (100 h at 400 °C and 30 MPa), it was found that a corrosion layer ranging from 150 to 480 μm formed due to oxidation in SCW (Ref 12). Furthermore, Al_2O_3 coating, applied by the spray pyrolysis process, reduced the weight change of T91 alloy by 9 times after 500 h SCW test at 500 °C and 25 MPa (Ref 13). Other oxide compounds such as CeO_2 - Ta_2O_5 and ZrO_2 - MgO were not as effective as Al_2O_3 in SCW (Ref 13).

A more comprehensive screening test of ceramic materials was carried out under acidic and oxidizing SCW conditions (465 °C, 25 MPa, 3% H_2O_2 , and 0.05 mol/kg HCl), different from that seen in SCWR, to find a suitable containment material for SCWO applications (Ref 14). Pure alumina (Al_2O_3) and sapphire samples showed excellent corrosion resistance, while mullite ($3\text{Al}_2\text{O}_3 \cdot 2\text{SiO}_2$)-based materials had inferior corrosion resistance compared to alumina. Ytria partially stabilized zirconia (Y-PSZ) samples exhibited poor corrosion resistance and disintegrated during testing due to the presence of impurities on the grain boundaries. Zirconia/magnesia samples were found to be corrosion resistant in that they exhibited no mass loss; however, the tetragonal ZrO_2 phase (about 30% in the zirconia/magnesia samples) transformed to monoclinic ZrO_2 during SCWO testing, causing volume expansion and subsequent cracking.

Among the available low thermal conducting ceramic materials, YSZ is so far the most promising candidate for SCWR as it has low neutron cross section, low thermal conductivity, good corrosion resistance in SCW (in the absence of H_2O_2 , HCl, or H_2SO_4) (Ref 15), and stability under neutron and ion irradiation conditions (Ref 16-18). Based on a preliminary calculation, assuming a thermal conductivity of 2.7 W/m K and 70% porosity, a minimum of 7 mm YSZ insulator is needed in order to limit the heat loss from the reactor core to the moderator to about 1.5% and effectively protect the pressure tube in a Canadian SCWR (Ref 3). The thickness of the insulator will increase if the temperature in the reactor core continues to rise. The

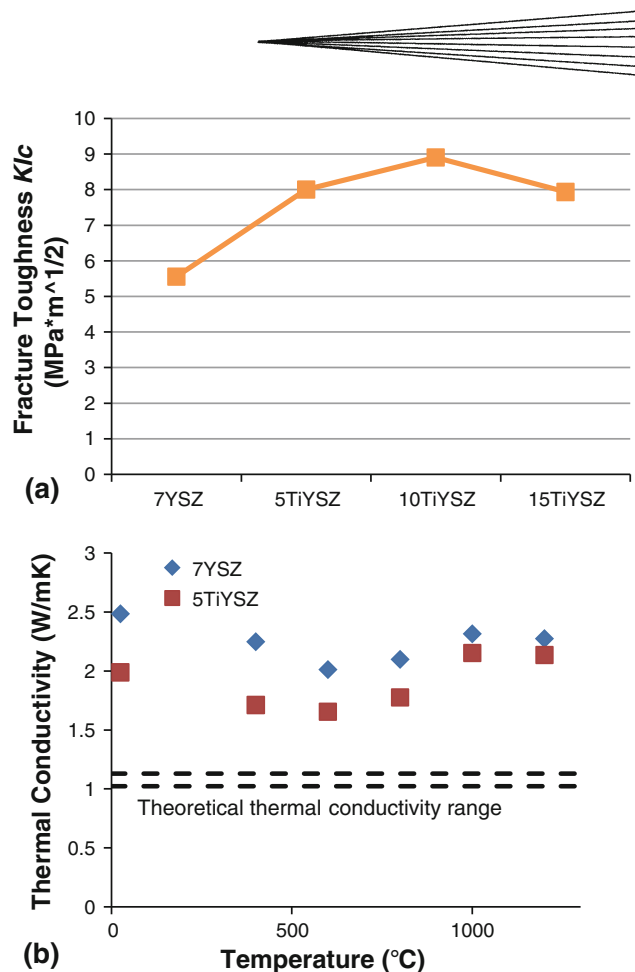


Fig. 2 Measured (a) fracture toughness of 7YSZ, 5TiYSZ, 10TiYSZ, and 15 TiYSZ and (b) thermal conductivity of 7YSZ and 5TiYSZ (Ref 19, 20)

use of 7YSZ faces several challenges: the increased thermal stress in a thick insulator due to thermal gradient, the cyclic load during start up and shut down operations, and the long-term phase stability of 7YSZ in SCW. Alternative materials [such as co-doped YSZ (Ref 19)] with lower thermal conductivity (to reduce the thickness and weight of the insulator), higher strength and toughness, more stable phases, and equivalent or superior corrosion resistance will provide more design options for the SCWRs.

This study was undertaken to evaluate the performance of several TiO_2 -doped 7YSZ ceramic materials (TiYSZ) in supercritical water. Our previous research has shown that the addition of TiO_2 increases the fracture toughness and reduces the thermal conductivity of 7YSZ (Fig. 2) (Ref 19, 20). TiO_2 also has the ability to stabilize tetragonal zirconia phase (Ref 21) and reduce the density. These properties make TiYSZ materials very attractive to SCWR application.

2. Experimental Procedures

2.1 Materials Preparation

Mild steel substrate (measured $1'' \times 4'' \times 0.059''$) was used as a sacrificial substrate for ceramic material deposition.

Table 1 Sample compositions

Sample ID	Powder designation	Composition, wt. %		Manufacturer
		(wt.%)	(mol%)	
Al ₂ O ₃	ALO-101	Al ₂ O ₃		Praxair
7YSZ	ZrO-271-3	ZrO ₂ , 7.5% Y ₂ O ₃		Praxair
TiO ₂	TIO-114	TiO ₂		Praxair
5TiYSZ	Mixture	5 wt.% TiO ₂ in 7YSZ	7.8	...
10TiYSZ	Mixture	10 wt.% TiO ₂ in 7YSZ	15	...
15TiYSZ	Mixture	15 wt.% TiO ₂ in 7YSZ	22	...

Table 2 Process parameters for Axial III plasma system

Parameters	Unit	Al ₂ O ₃	7YSZ/TiYSZ
Argon	%	0	0
Nitrogen	%	75	75
Hydrogen	%	25	25
Total flow rate	slpm	250	250
Powder deed rate	g/min	~31	~50
Carrier gas flow rate	slpm	12	12
Current	A	250	250
Nozzle size	in.	3/8	3/8
Spray distance	mm	150	150
Duration of coating run	min	4	7
Turntable rotation speed	rpm	220	220
Turntable vertical cycle rate	ipm	40	40

Table 3 Test parameters

Autoclave run	Test stage	Temp., °C	Pressure start/end, MPa	Time, h	DO level, ppm	pH value (before/after)
Run 1 (Al ₂ O ₃ and 7YSZ)	Stage 1	500	27.5/25.9	500	1.0	5/5
	Stage 2	500–540	27.8/22.4	440	0.6	5/5
Run 2 (5TiYSZ, 10TiYSZ and 15TiYSZ)	Stage 1	500	27.8/24.9	486	0.5	5/5
	Stage 2	502	26.6/23.0	690	1.0	5/5

Since no commercial TiO₂-doped YSZ powder material was available in the market, a plasma spraying process followed by sintering was used as the means to produce consolidated bulk samples for this study. The deposition was carried out using an Axial III Plasma Spray System (Northwest Mettech, Vancouver, BC, Canada). All powder materials were purchased from Praxair Inc. with powder designations and compositions listed in Table 1. 5TiYSZ, 10TiYSZ, and 15TiYSZ represent samples with 5, 10, and 15 wt.% TiO₂ added to 7YSZ (equivalent mol% of TiO₂ in 7YSZ was also calculated and provide in the Table 1). Mechanical alloying with a ball mill (Planetary Mono Mill Pulverisette 6, Fritsch GmbH) was utilized to produce powder mixtures containing TiO₂ and 7YSZ. The milling process was experimentally derived (check for powder size after every 5 min milling) so that only limited grinding took place. The parameters for the plasma spray process are summarized in Table 2. A series of plasma spray trials was conducted using 7YSZ powder. The parameters that provided the highest coating density and spray efficiency (μm/s) were selected for this study (Ref 22).

In addition to TiO₂-doped 7YSZ samples, two reference materials, Al₂O₃ and 7YSZ, were also plasma-sprayed on

to the mild steel substrate as alumina is a common ceramic material used in a supercritical water oxidizing (SCWO) system and 7YSZ is being considered as a potential thermal insulation material for SCWR. After plasma spraying, the ceramic materials were separated from the mild steel substrate in order to test them in a SCW autoclave. This was accomplished using a nitric acid etching method. After the removal of sacrificial mild steel substrate, the samples were further sintered at 1100 °C for 500 h. This was carried out to homogenize the composition and also in an attempt to consolidate the plasma-sprayed materials. According to the calculated isothermal sections of the TiO₂-YO_{1.5}-ZrO₂ system (Ref 23), TiYSZ samples are estimated to be in the single t phase region between 1000 and 1200 °C.

After sintering, square sample pieces of roughly 1 cm × 1 cm were broken off and both sides were polished with 600 grit sand paper (a standard procedure to prepare samples for SCW testing) to give a nominal thickness of 0.45 mm. The final step before their placement in the autoclave was a thorough cleaning in an ultrasonic bath with distilled water. The samples were then baked at 200 °C for 2 h before being weighed. For comparison purposes, two sets of samples were prepared

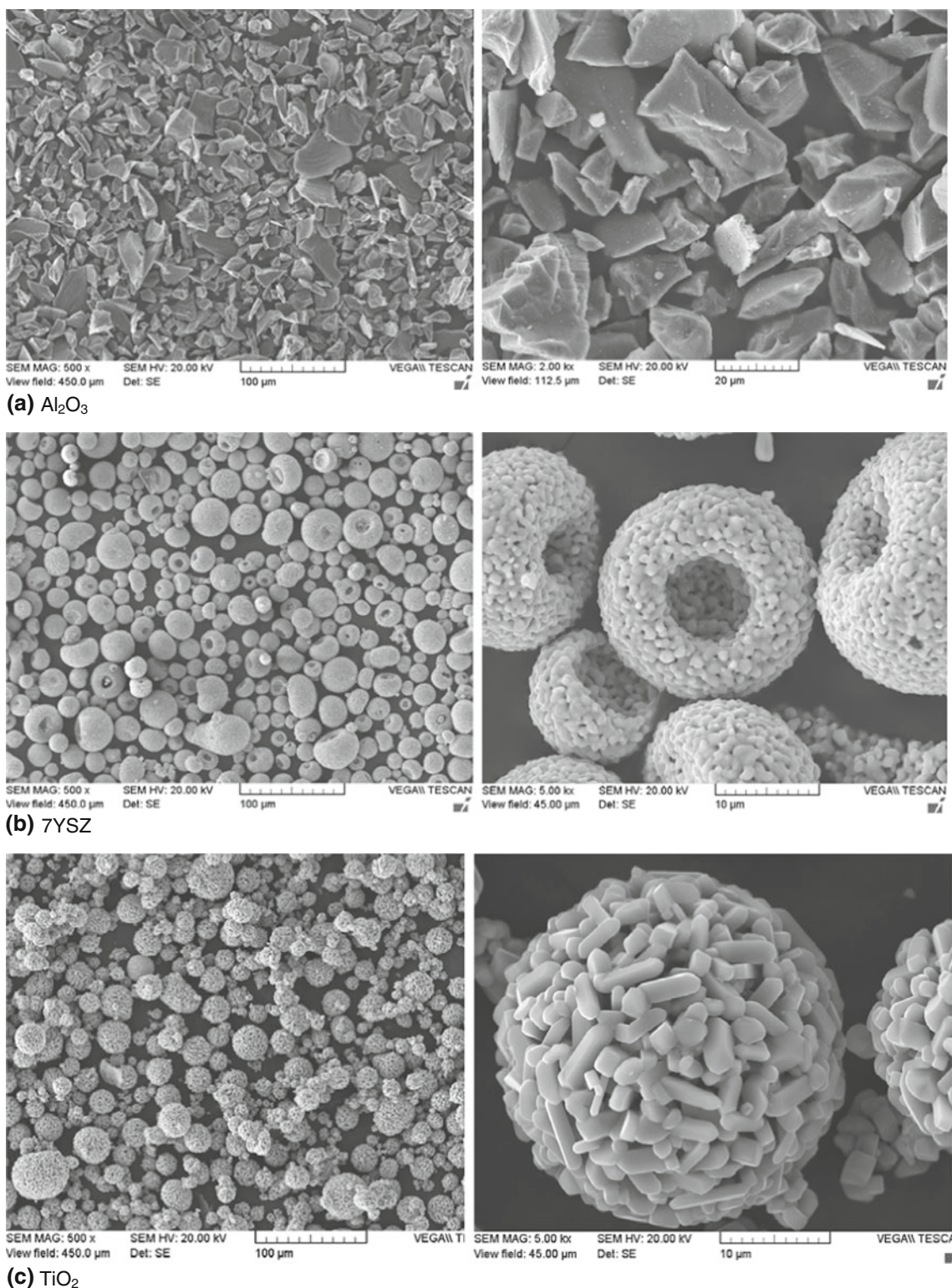


Fig. 3 Powder morphology of starting powders at 500 \times (left) and 5000 \times magnification (right). (a) Al₂O₃. (b) 7YSZ. (c) TiO₂

with one set remaining in the as-prepared condition and the other set subjected to the SCW test.

As a silicone-based substance was found on samples tested previously in the SCW autoclaves (due to the use of

silicone sealant), all ceramic samples examined in this study were ultrasonically cleaned in alkaline solution followed by a silicon removal agent to remove the contamination before weighing and SEM examination.

2.2 Testing Procedure

Two autoclaves (Parr model 4650, Parr Instrument, USA), controlled by a model 4838 Parr reactor/autoclave controller, were used in this study for runs 1 and 2. Once samples were loaded into the pressure vessel, a vacuum was drawn and a predetermined quantity of water was injected via a self-sealing rubber plug. The quantity of water was calculated based on the volume of the vessel minus the volume of all samples and sample holder, the temperature, and the desired pressure. The Parr data logging system kept track of the conditions (temperature and pressure) during the experiment. A water sample was taken at the start and end of each stage of the experiment and the dissolved oxygen (DO) and pH value were measured. The experiment was accomplished in two stages due to a leakage in the pressure vessel. Table 3 provided details of the test conditions. At the end of stage 2, all samples were weighed using a scale (Acculab, Satorius) with a precision of 0.0001 g.

The microstructure of the as-tested sample surface (polished with 600 grit sand paper), before the SCW test, and cross section was evaluated using Scanning Electron Microscopy (SEM) (Vega II XMU, Tescan) and Energy Dispersive X-ray Spectrometry (EDS) (INCA-X, Oxford Instruments). The phase composition of the sintered TiYSZ samples was analyzed by an X-ray diffractometer (Bruker D8 Powder). During XRD analysis, a CoK_α radiation X-ray source was used with an applied voltage

and a current of 35 kV and 40 mA. All tests were carried out within a 2θ range of 30-90 degrees (θ is the angle between the incident X-ray beam and the horizontal surface of the sample).

3. Results

3.1 Powder Morphologies of Al_2O_3 , 7YSZ, and TiO_2

The alumina powder had an irregular shape with powder size distribution in the range of 5 to 50 μm . The 7YSZ and TiO_2 powders were made of sintered particles with a more uniform powder size distribution of 10-40 μm . The morphologies of the original powders before mechanical alloying are shown in Fig. 3(f).

3.2 XRD Analysis of TiYSZ Samples

The sintered TiYSZ samples were analyzed by XRD to determine the phase compositions. The XRD results showed that all TiYSZ samples contained less than 2.5 mol% monoclinic phase and they were made primarily of tetragonal phase (>83 mol%). Although not measured quantitatively, traces of possible rutile (R- TiO_2) or pyrochlore phases (Ref 24) could be present in the TiYSZ samples as shown in the XRD spectra (Fig. 4).

3.3 Visual Inspection of Samples After SCW Testing

Before and after SCW testing, samples were visually inspected. Differences in shading were observed for Al_2O_3 samples which had a light cream color before testing and turned a whitish shade after SCW testing. 7YSZ samples had a similar whitish color before and after testing, while all TiYSZ samples changed from a gray to a slightly darker gray after SCW testing. Also noted on the 7YSZ samples were small hairline cracks before and after SCW testing. The occurrence of these hairline cracks is believed to be as a result of the stress generated during the sintering and polishing processes. SEM analysis (Fig. 7) will provide more details on the surface cracking of 7YSZ samples.

3.4 Weight Changes

The weight changes after testing for approximately 1000 h were measured and the average rate of weight change, as a relative scale to compare material dissolution/addition in SCW per unit time, is included in Table 4 and Fig. 5.

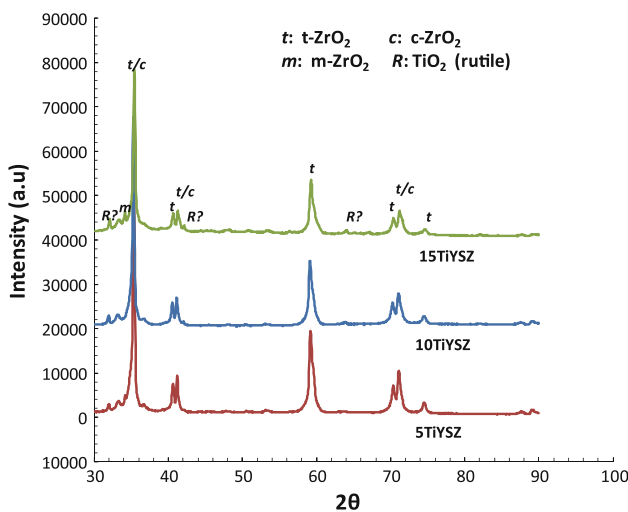


Fig. 4 XRD patterns of 5TiYSZ, 10TiYSZ, and 15TiYSZ after sintering

Table 4 Weights before and after SCW testing

ID	Weight before testing, g	Weight after testing, g	Surface area, cm^2	Average rate of weight change, mg cm^{-2} per hour
Al_2O_3	0.076	0.0770 (940 h)	0.6414	0.00166
7YSZ	0.1135	0.1136 (940 h)	0.8729	0.00012
5TiYSZ	0.2222	0.2221 (1176 h)	1.7911	-0.00005
10TiYSZ	0.143	0.1430 (1176 h)	1.1176	0.00000
15TiYSZ	0.1712	0.1714 (1176 h)	1.3910	0.00012

From the test results, it was found that the average rate of weight change followed an order of $\text{Al}_2\text{O}_3 > 7\text{YSZ}$, $15\text{TiYSZ} > 10\text{TiYSZ} > 5\text{TiYSZ}$. More importantly, one TiO_2 -doped sample (10TiYSZ) showed zero weight change after 1176 h of testing. Although 5TiYSZ saw a slight weight loss, the amount of weight change was close to the precision limit of the scale used. Overall, the TiYSZ samples showed improved or equivalent performance as 7YSZ in terms of sample weight change.

3.5 Surface and Cross Section Microstructure

Samples were examined using SEM and EDS after SCW testing. Figures 6-8 present the surface microstructure of all samples. Figures 8 and 9 provide the cross-sectional view of TiYSZ samples after SCW testing. The Al_2O_3 samples showed very similar surface features before and after SCW testing, apart from the presence of several bright contaminant particles (Si-containing particles from the silicone sealant used in autoclaves) in Fig. 6(b). The voids seen in Fig. 6(a) and (b) are from the plasma spray process.

The 7YSZ sample after the second stage of SCW testing showed apparent surface cracking (Fig. 7(a)) and

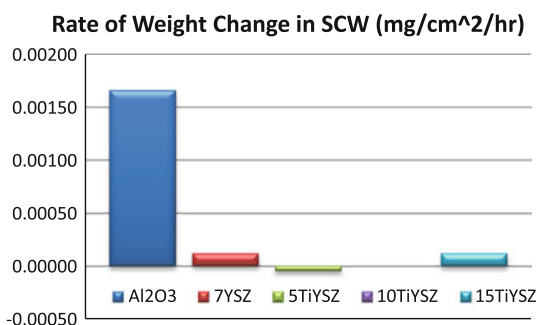


Fig. 5 Rate of weight change for Al_2O_3 , 7YSZ, 5TiYSZ, 10TiYSZ, and 15TiYSZ

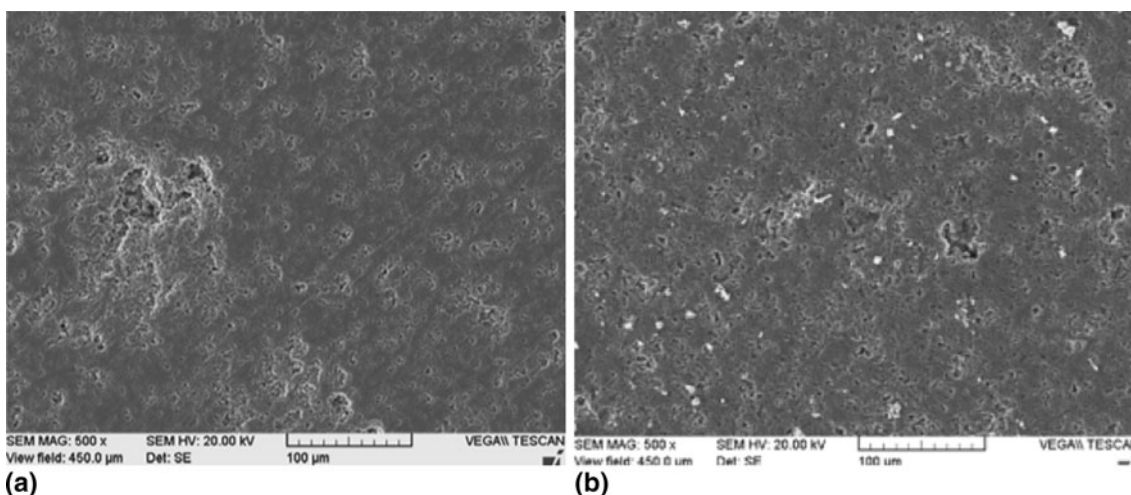


Fig. 6 Surface morphology of Al_2O_3 before (a) and (b) after SCW testing (stage 2)

occasional surface contaminants (see boxed region in Fig. 7(b)). Examining the cracked area at high magnification, it was found that the crack (pointed by arrows) was several micrometers wide and the regions adjacent to the crack were more porous than the bulk of the sample. The 7YSZ sample in the as-prepared state (not tested in SCW) was further examined and similar cracks were observed. These cracks were likely to have formed during sample preparation (cooling from sintering and polishing), suggesting a brittle nature of the material.

The three TiO_2 -doped samples (5TiYSZ, 10TiYSZ, and 15TiYSZ) showed similar surface features (Fig. 7(b)-(d)): small black pin holes and polishing lines on the otherwise smooth surface. No cracks were observed on these samples. When examined under higher magnification, all TiYSZ samples contained light Si-containing discrete particles in the boxed regions. Samples 10TiYSZ and 15TiYSZ also had pockets of needle-shaped phases in the circled regions in Fig. 8(a) and (b). The size of these needle-shaped particles matches that of the original TiO_2 power particles. And, XRD analysis also showed the presence of possible R- TiO_2 (rutile) after sintering (Fig. 4). The existence of these needle-shaped particles could be either due to the incomplete dissolution of TiO_2 in 7YSZ on sample surfaces or due to cooling from high temperature sintering as the solid solution limit of TiO_2 in 7YSZ at room temperature may have been exceeded for 10TiYSZ and 15TiYSZ (containing about 15 and 22 mol% of TiO_2 , respectively). Also found on the surfaces of 10TiYSZ and 15TiYSZ were minute light particles in the boxed regions of Fig. 8. These particles were too fine to be analyzed with EDS analysis or X-ray mapping.

SEM examination of the cross sections of SCW-tested samples did not reveal the presence of any surface pitting or corrosion product. The microstructure of TiYSZ samples, illustrated in Fig. 9, still resembles the as-sprayed lamellar structure with some remaining pores. Fine grains

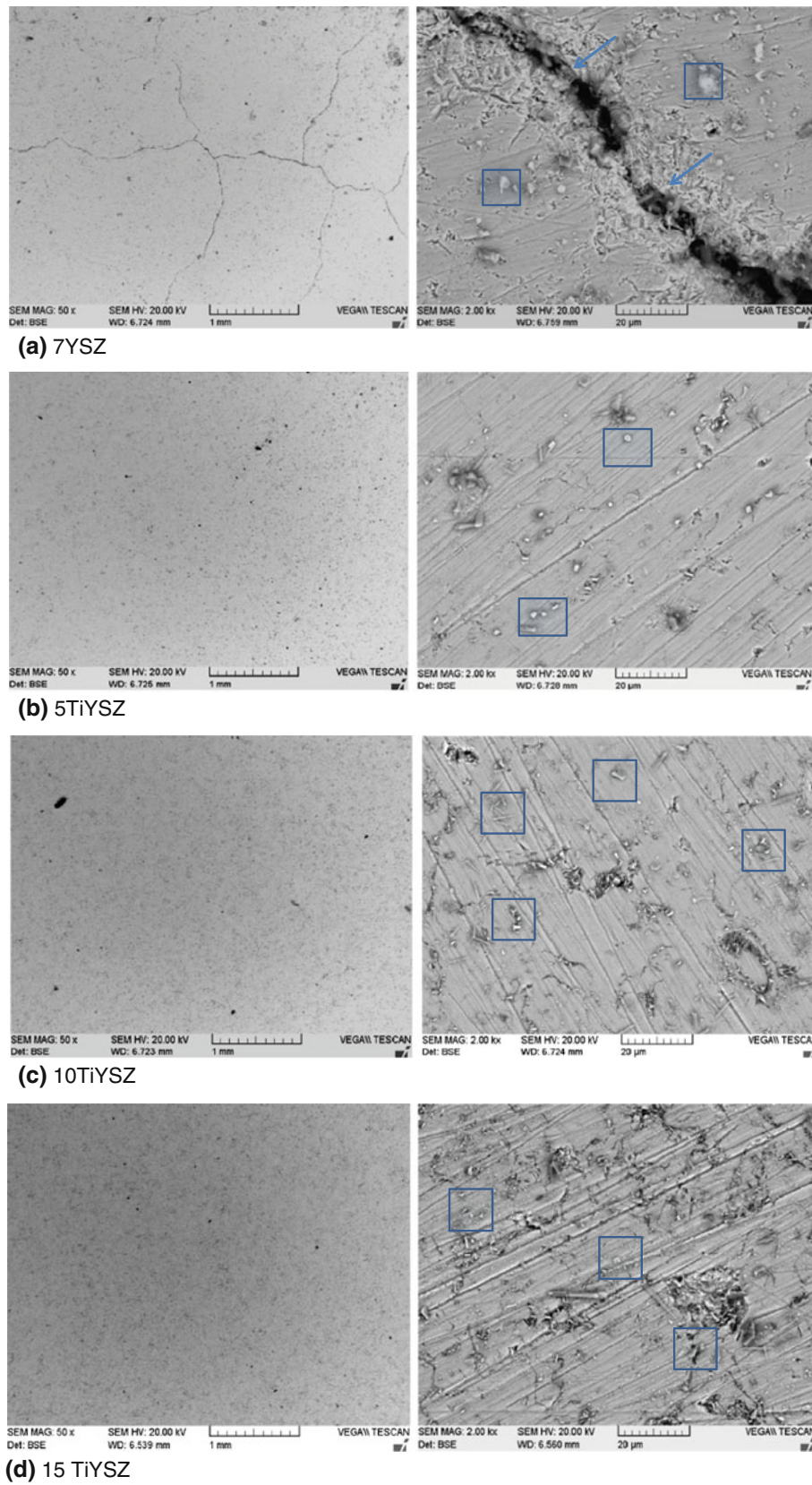


Fig. 7 SEM images of 4 samples after SCW testing. (a) 7YSZ, (b) 5TiYSZ, (c) 10TiYSZ, and (d) 15TiYSZ (note that the images shown here were taken from the surfaces of the as-tested samples)

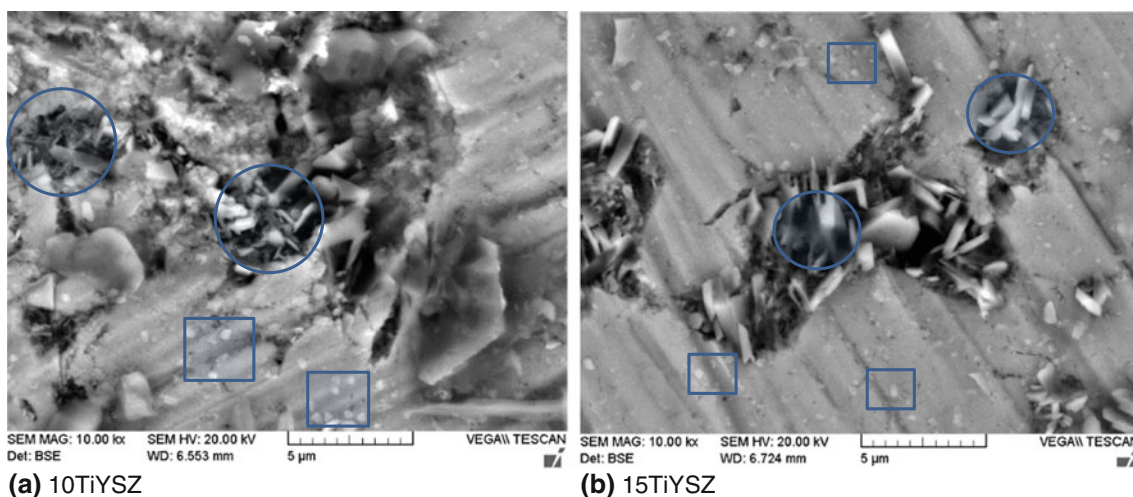


Fig. 8 Enlarged views of 10TiYSZ (a) and 15% TiYSZ (b). Possible TiO₂ and surface contaminants are found in circled and boxed regions, respectively

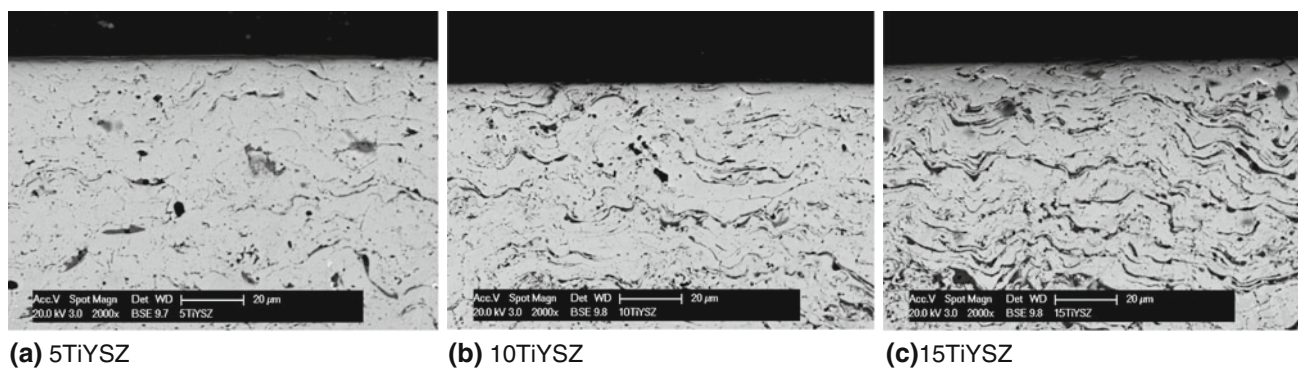


Fig. 9 Cross sections of 5TiYSZ (a), 10TiYZ (b), and 15TiYSZ (c) after SCW testing

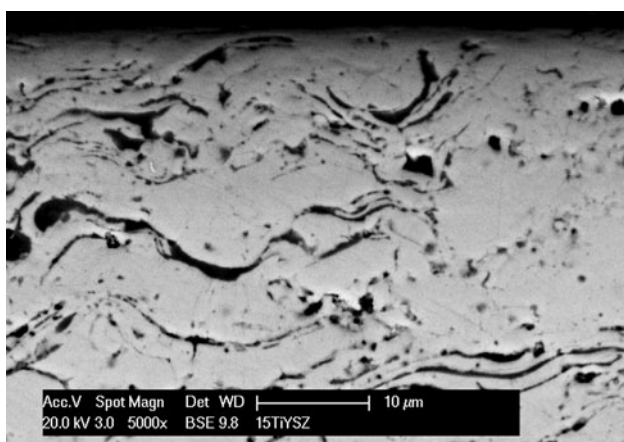


Fig. 10 Cross section of 15TiYSZ

are also observed in the sintered structure (Fig. 10). Needle-shaped particles were not observed on the cross sections of 5TiYS, 10TiYZ, and 15TiYSZ.

4. Discussion

Weight change was used in this preliminary study of TiYSZ to provide indications of a possible reaction between each test sample and SCW. Since samples were not tested to exactly the same amount of time, the weight change was normalized to give the rate of weight change. When weight loss is observed, it signifies material removal by dissolution, evaporation, or reduction. Excessive weight loss is always detrimental to component integrity and also has the potential to contaminate the working fluid. In the present study, no substantial weight loss was found in all tested samples.

In a case where weight gain is observed, it can indicate oxidation (oxide formation on the surface adds weight), hydration, or other corrosion products formed on the surface. The formation of these compounds is usually undesirable as the base material is being consumed. However, if a dense, adherent surface scale can be formed (such as alumina on NiCrAlY alloys or chromia on stainless steels), it is beneficial in terms of preventing

further consumption of the base material. In this study, weight gain was observed for the alumina sample and this could be attributed to the possible hydration of alumina in SCW. In fact, a previous study has found that sputter-deposited alumina formed $\text{Al}_2\text{O}_3 \cdot (\text{H}_2\text{O})_{1.5}$ when being exposed to deionized water (Ref 24).

The other four samples (7YSZ, 5TiYSZ, 10TiYSZ, and 15TiYSZ) showed minimal or no weight change. This suggests two possibilities. One is that these materials are resistant to the environment. No reaction took place during SCW test. However, negligible or no weight change can also result from simultaneous material removal and scale formation. As such, it is important that the tested surface be examined to determine if there is any scale formation. The cross section examination did not reveal any surface pitting or scale formation on all samples (examples of which are shown in Fig. 9). It is thus confirmed that very limited or no reaction with SCW occurred during testing of 5TiYSZ, 10TiYSZ, and 15TiYSZ.

5. Conclusion and Future Work

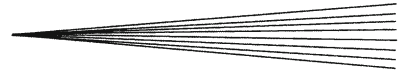
In this preliminary study, three TiO_2 -doped 7YSZ samples and two reference materials, Al_2O_3 and 7YSZ, were tested under SCW condition for approximately 1000 h. The rate of weight change was used to rank different materials in terms of their corrosion resistance in SCW. Minimal weight change combined with the lack of surface scale formation provided an indication of resistance to SCW attack. The results showed that Al_2O_3 experienced some weight gain, possibly due to hydration. The weight changes for 7YSZ and 15TiYSZ were much less than Al_2O_3 and 5TiYSZ and 10TiYSZ showed negligible weight change. Cracks were found on 7YSZ samples before and after SCW testing, indicating the relatively brittle nature of the material. For 10TiYSZ and 15TiYSZ, possible R- TiO_2 clusters were found on the sample surface due to either incomplete dissolution or limited solid solution in 7YSZ. The results obtained so far suggest that the addition of TiO_2 to 7YSZ has the advantages of increasing fracture toughness and reducing thermal conductivity, while at the same time showing an equivalent rate of weight change in SCW to 7YSZ. Should TiO_2 -doped 7YSZ be used in SCWR, the foreseeable benefits include reduced insulation thickness, resistance to thermal shock, lighter weight, and phase stability due to the stabilization of the tetragonal phase. A future study with pre-alloyed plasma spray powder should be conducted to obtain more homogeneous microstructure and eliminate the possible effect of a trace amount of secondary phases on the general properties and corrosion behavior.

Acknowledgment

Financial support for material and test equipment was provided by the NSERC/NRCAN/AECL under a NSERC CRD research grant.

References

1. T. Richard, J. Poirier, C. Reverte, C. Aymonier, A. Loppinet-Seranic, G. Iskender, E. Pablo, and F. Marias, Corrosion of Ceramics for Vinasse Gasification in Supercritical Water, *J. Eur. Ceram. Soc.*, 2012, **32**, p 2219-2233
2. M. Schacht, N. Boukis, and E. Dinjus, Corrosion of Alumina Ceramics in Acidic Aqueous Solutions at High Temperatures and Pressures, *J. Mater. Sci.*, 2000, **35**, p 6251-6258
3. C. Chow and H. Khartabil, Conceptual Fuel Channel Designs for CANDU-SCWR, *Nucl. Eng. Technol.*, 2007, **40**(2), p 139-146
4. S. Baidur, Materials Challenges for the Supercritical Water Cooled Reactor (SCWR), *Bull. Can. Nucl. Soc.*, 2008, **29**(1), p 32-38
5. L. Leung, Canada's Super-Critical Water-cooled Reactor Design Concept, Phase-II NSERC/NRCAN/AECL Gen-IV Energy Technologies Program Kick-Off Meeting, Saskatoon, Canada, June 14, 2012
6. C. Chow and H.F. Khartabil, Conceptual Fuel Channel Designs for CANDU – SCWR, *Nucl. Eng. Technol.*, 2007, **40**(2), p 139-146
7. P. Kritzer, Corrosion in High-Temperature and Supercritical Water and Aqueous Solutions: A Review, *J. Supercrit. Fluids*, 2004, **29**, p 1-29
8. Y.-J. Kim and P.L. Andresen, Application of Insulated Protective Coatings for Reduction of Corrosion Potential of Type 304 Stainless Steel in High-Temperature Water, *Corrosion*, 1998, **54**(12), p 1012-1017
9. D.A. Guzonas, J.S. Wills, G.A. McRae, S. Sullivan, K. Chu, K. Heaslip, and M. Stone, *12th International Conference on Environmental Degradation of Materials in Nuclear Systems – Water Reactors*, Salt Lake City, 14-18 August 2005
10. J. Wills, D.A. Guzonas, and A. Chiu, *28th Annual CNS Conference*, Saint John, 2007
11. C. Sun, R. Hui, W. Qu, and S. Yick, Progress in Corrosion Resistant Materials for Supercritical Water Reactors, *Corros. Sci.*, 2009, **51**, p 2508-2523
12. X. Yi, A. Yamauchi, K. Kurokawa, and T. Akiyama, Corrosion of Combustion-Synthesized β -SiAlONs in Supercritical Water, *Corros. Sci.*, 2012, **56**, p 153-157
13. C. Sun, Y. Xie, P. Yao, L. Zhang, J. Miles, W. Cook and R. Hui, *2nd Canada-China Joint Workshop on SCWR (CCSC-2010)*, Toronto, ON, Canada, 25-28 April 2010
14. N. Boukis, N. Claussen, K. Ebert, R. Janssen, and M. Schacht, Corrosion Screening Tests of High-Performance Ceramics in Supercritical Water Containing Oxygen and Hydrochloric Acid, *J. Eur. Ceram. Soc.*, 1997, **17**(1), p 71-76
15. B. Savoini, D. Cáceres, I. Vergara, R. González, and J.E. Santiuste, Radiation Damage in Neutron-Irradiated Yttria-Stabilized-Zirconia Single Crystals, *J. Nucl. Mater.*, 2000, **277**(2-3), p 199-203
16. T. Hojo, J. Aihara, K. Hojou, S. Furuno, H. Yamamoto, N. Nitani, T. Yamashita, K. Minato, and T. Sakuma, Irradiation Effects on Yttria-Stabilized Zirconia Irradiated with Neon Ions, *J. Nucl. Mater.*, 2003, **319**, p 81-86
17. K.E. Sickafus, H. Matzke, K. Yasuda, P. Chodak, III, R.A. Verrall, P.G. Lucuta, H.R. Andrews, A. Tuross, R. Fromknecht, and N.P. Baker, Radiation Damage Effects in Cubic-Stabilized Zirconia Irradiated with 72 MeV I^+ Ions, *Nucl. Instrum. Methods Phys. Res. B*, 1998, **141**(1-4), p 358-365
18. C. Degueldre and Ch. Hellwig, Study of a Zirconia Based Inert Matrix Fuel Under Irradiation, *J. Nucl. Mater.*, 2003, **320**(1-2), p 96-105
19. M. Kibsey, J. Romualdez, X. Huang, R. Kearsey, and Q. Yang, Mechanical Properties of Titania-Doped Yttria Stabilized Zirconia (TiYSZ) for Use as Thermal Barrier Coating (TBC), *ASME J. Eng. Gas Turbines Power*, 2011, **133**(12), p 122101-122110
20. J. Romualdez, M. Kibsey, X. Huang, and R. Kearsey, *Thermal Properties and Phase Analysis of Titania Doped Yttria-Zirconia Ceramics for Use as High Temperature Thermal Barrier Coatings (TBCs)*, Turbo Expo 2011, Paper No. GT2011-45054, Vancouver, June 2010



21. T.A. Schaedler, R.M. Leckie, S. Krämer, A.G. Evans, and C.G. Levi, Toughening of Nontransformable t' -YSZ by Addition of Titania, *J. Am. Ceram. Soc.*, 2007, **90**(12), p 3896-3901
22. F. Gao, X. Huang, Q. Yang, and R. Liu, Optimization and Prediction of Plasma Spray Process by Taguchi Method, *J. Therm. Spray*, 2012, **21**(1), p 176-186
23. T.A. Schaedler, O. Fabrichnaya, and C.G. Levi, Phase Equilibria in the TiO_2 - $\text{YO}_{1.5}$ - ZrO_2 system, *J. Eur. Ceram. Soc.*, 2008, **28**, p 2509-2520
24. M.O. Jarligo, G. Mauer, D.E. Mack, R. Vaßen, and D. Stöver, *Proceedings of the 25th International Conference on Surface Modification Technologies (SMT 25)*, T.S. Sudarshan and P. Nylén, Ed., June 20-22, 2011, Valardocs, Trollhättan, Sweden, January 2012, p 165-173
25. T. Kawabe, M. Hanazono, Y. Sono, M. Waki, and S. Hara, *Proceedings of the Symposium on Dielectric Films on Compound Semiconductors*, Honolulu, HI, USA, Oct. 18-23, 1988, p 217-222